npg

ORIGINAL ARTICLE

Overexpressing the *CCL2* chemokine in an epithelial ovarian cancer cell line results in latency of *in vivo* tumourigenicity

P Wojnarowicz[1], K Gambaro[1], M de Ladurantaye[2], MCJ Quinn[2], D Provencher[2,3,4], A-M Mes-Masson[2,5] and PN Tonin[1,6,7]

The frequent loss of heterozygosity of chromosome (Chr) 17 in epithelial ovarian cancer (EOC), particularly high-grade ovarian serous carcinomas (HGOSCs), has been attributed to the disruption of known tumour suppressor genes, such as *TP53* (17p13), as well as other genes on this chromosome that alone or in combination have a role in EOC. In a transcriptome analysis of Chr17 genes, we observed significant underexpression of the chemokine *CCL2* (17q12) in a small set of HGOSC samples relative to normal ovarian surface epithelial cells and a significant upregulation of *CCL2* in the *TP53*-mutated OV-90 EOC cell line rendered non-tumourigenic as a consequence of genetic manipulation. Here, we report that overexpressing *CCL2* in OV-90 resulted in latency of tumour formation at intraperitoneal (i.p.) but not subcutaneous sites in a mouse xenograft model. Overexpressing *CCL2* affected cell morphology and exerted modest, but not significant effects on cell viability, colony formation and cell migration. We report significant underexpression of *CCL2* by transcriptome analysis ($P = 0.015$) and by immunohistochemistry in 77% of HGOSC samples ($n = 65$). Absent or a very low level of protein expression by immunohistochemistry was also observed in 71% of additional HGOSC samples ($n = 122$). However, CCL2 protein expression did not significantly correlate with overall or disease-free survival. The epithelial cells of normal fallopian tubes, a purported origin of HGOSC, exhibited expression of CCL2 protein by immunohistochemistry. Our results affirm that *CCL2* underexpression is a significant feature of HGOSC samples, and that *CCL2* overexpression in an EOC cell line model affects tumourigenic potential in the i.p. setting.

INTRODUCTION

A well-documented feature of epithelial ovarian cancers (EOCs) is the high frequency of loss of heterozygosity of a chromosome (Chr) 17 contig.[1–5] This observation along with complementation studies showing a reduction in tumourigenicity of an EOC cell line harbouring a transferred normal Chr17,[6] have suggested that Chr17 harbours tumour suppressor genes (TSGs). Chr17 TSGs implicated in EOC include *TP53* the most frequently mutated gene in EOC, and *BRCA1*, where a germline mutation predisposes to hereditary EOC.[7–13] Recently *DPH1*, *HIC1*, *NF1*, *RARA*, *RHBDF2* and *CYGB* have been proposed as TSGs in EOC, suggesting that a number of Chr17 genes have a role in EOC.[14–18]

In a recent transcriptome analysis, we described Chr17 genes dysregulated in high-grade ovarian serous carcinomas (HGOSCs) as compared with normal ovarian surface epithelial cells (NOSEs),[19] and showed that the chemokine *CCL2* (17q12) was one of the genes significantly underexpressed in HGOSCs.[19] We also reported low or absent expression in tumourigenic EOC cell lines as compared with a non-tumourigenic EOC cell line.[19] Low or absent *CCL2* expression in EOCs and cell lines has also been reported independently.[20–22] Underexpression has not been attributed to aberrant promoter methylation or somatic mutations.[20] Interestingly, single-nucleotide polymorphisms, located proximal

to the *CCL2* locus, have been associated with risk for survival in OSCs.[23] *CCL2* was also shown significantly underexpressed in chemoresistant EOCs as compared with chemosensitive samples, and increased expression was an independent predictor of complete response, chemosensitivity and progression-free survival.[24] This group also reported that overexpressing *CCL2* in a chemosensitive EOC cell line resulted in increased *in vitro* sensitivity to paclitaxel.[24] In all of these studies gene expression analyses were limited by sample size and thus it is not clear whether dysregulated *CCL2* expression is characteristic of HGOSC, which may signify a role in disease pathology.

CCL2 encodes a member of the C–C subfamily of chemokines, which functions as a chemoattractant for monocytes, memory T lymphocytes and natural killer (NK) cells.[25] The role of *CCL2* in cancer appears to be complex, as *CCL2* has been shown to both promote and suppress tumourigenicity. In gastric carcinoma cells, *CCL2* expression increased tumourigenesis and induced metastasis, whereas in malignant CHO cells, *CCL2* expression suppressed tumour formation.[26,27] In a melanoma cell line, *CCL2* expression led to tumour destruction but only with high levels of gene expression, while intermediate levels resulted in increased angiogenesis and tumour growth.[28] Interestingly, we have observed that *CCL2* expression was significantly induced in an

[1]Department of Human Genetics, McGill University, Montreal, Canada; [2]Centre de recherche du Centre hospitalier de l'Université de Montréal (CRCHUM)/Institut du cancer de Montréal, Montreal, Canada; [3]Division de gynécologie oncologique, Université de Montréal, Montreal, Canada; [4]Départment d'obstetriques et gynécologie, Université de Montréal, Montreal, Canada; [5]Département de médicine, Université de Montréal, Montreal, Canada; [6]The Research Institute of the McGill University Health Centre, Montreal, Canada and [7]Department of Medicine, McGill University, Montreal, Canada. Correspondence: Dr PN Tonin, Medical Genetics, Montreal General Hospital, Room L10-132, 1650 Cedar Avenue, Montreal, Quebec, Canada H3G 1A4.
E-mail: patricia.tonin@mcgill.ca
Received 10 May 2012; revised 29 June 2012; accepted 3 July 2012

EOC cell line, OV-90, which was rendered non-tumourigenic as a consequence of Chr3 fragment transfer in the context of a genetic complementation assay aimed at identifying genes implicated in TSG pathways.[29,30] Transcriptome analyses showed that *CCL2* was one of the most significantly upregulated genes in OV-90 Chr3-derived hybrids in addition to global transcriptome alterations that had occurred which when integrated with the transcriptomes of HGOSC samples, suggested that biological networks characteristic of HGOSC were affected.[29,30] How *CCL2* expression intersects TSG pathways is unknown, as the generation of stable *CCL2*-expressing clones from EOC cell lines that do not express *CCL2* have been unsuccessful.[20] Thus, the effect of modulating *CCL2* expression on the tumourigenic potential of EOC cells is unknown.

To investigate the effect of *CCL2* expression on the tumourigenic potential of EOC cells, we generated *CCL2*-expressing clones of the well-characterized OV-90 EOC cell line.[31] OV-90 exhibits morphological and somatic genetic features characteristic of HGOSC, such as harbouring a *TP53* mutation and chromosomal anomalies involving Chr17.[31] OV-90 does not express *CCL2* and is tumourigenic in mouse xenograft models.[31] Moreover, as referred to above, we have reported that *CCL2* expression was significantly induced in OV-90 clones that were rendered non-tumourigenic as a consequence of genetic manipulation.[29,30] Here, we report the effect of *CCL2* overexpression on the *in vitro* growth characteristics and *in vivo* tumourigenic potential of the OV-90 cell line. Another objective of our study was to describe *CCL2* gene and protein expression in an expanded set of well-defined HGOSCs and in normal tissues, particularly epithelial cells of normal fallopian tubes, one of the purported origins of HGOSC. As clinical correlates were available for HGSOC samples examined, we also relate expression to overall and disease-free survival.

RESULTS

Generation of OV-90 clones expressing CCL2

To assess the biological effect of expressing *CCL2* in EOC, we transfected OV-90 with a pDream2.1:*CCL2* construct. *CCL2* gene and protein expression in OV-90 are undetectable by reverse transcription (RT)–PCR and enzyme-linked immunosorbent assay analyses (ELISA) (Figures 1a and b). Two OV-90 clones, OV-90:*CCL2*[23] and OV-90:*CCL2*[49], were selected from the 47 clones obtained in cell transfection assays with the *CCL2*-expressing construct. They were selected for further analysis based on the high level of CCL2 protein and gene expression as compared with RH-6 and the parental OV-90 cell line (Figures 1a and b, Supplementary Table S1). RH-6 is one of the OV-90 hybrids derived in previous chromosome transfer experiments that demonstrated transcriptional reprogramming, including upregulation of *CCL2*, and suppression of tumourigenic potential as compared with OV-90.[29] The effect of overexpressing *CCL2* in the OV-90:*CCL2* clones was compared with the parental OV-90 cell line and two 'empty vector' (EV) clones, OV-90:EV[2] and OV-90:EV[9], selected from the 16 OV-90 clones transfected with pDream2.1, that also demonstrated no evidence of *CCL2* expression (Figures 1a and b).

In vitro morphological and growth characteristics of *CCL2*-expressing clones

In cell culture, OV-90 propagates as a homogeneous monolayer of tightly packed cells with a cobblestone-like appearance typified by epithelial cells[31] (Figure 1c). In contrast, the cell morphology of the *CCL2*-expressing clones, particularly OV-90:*CCL2*[23], appeared more elongated and the individual cells were less tightly packed as compared with OV-90 and the EV clones (Figure 1c).

The clones exhibited no overt differences in growth rate as they were passaged in cell culture. Though the viability of all clones
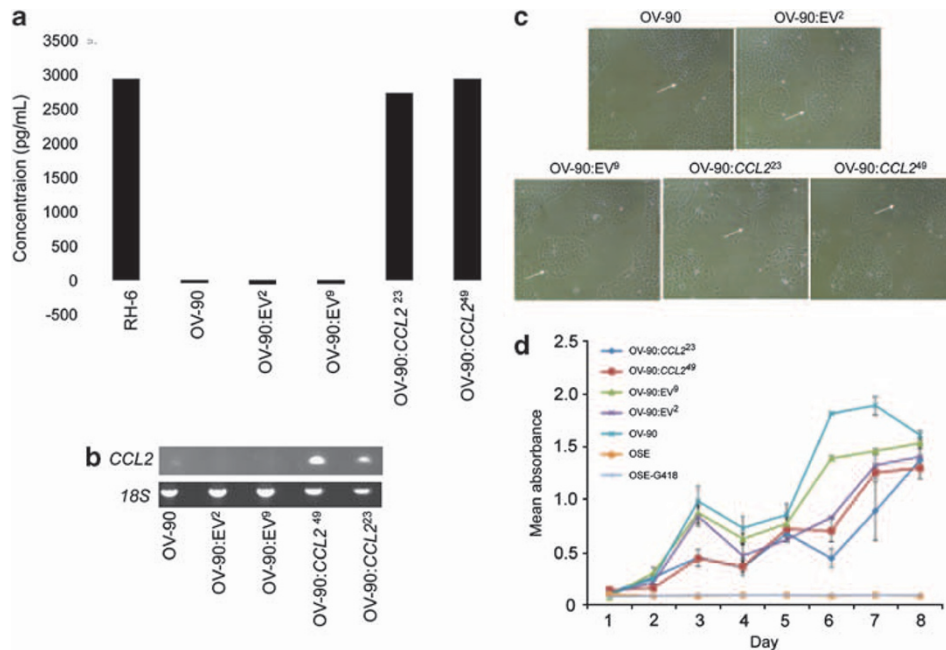

Figure 1. Characterization of *CCL2*-expressing clones. CCL2 ELISA results for a positive control (RH-6), a negative control (OV-90), stable EV clones: OV-90:EV[2], OV-90:EV[9], and stable *CCL2*-expressing clones: OV-90:*CCL2*[23] and OV-90:*CCL2*[49] (**a**). Semi-quantitative RT–PCR analysis of *CCL2* performed on complementary (c) DNA samples prepared from the parental OV-90, OV-90:EV[2], OV-90:EV[9], OV-90:*CCL2*[23] and OV-90:*CCL2*[49] (**b**). The expression of *18S* cDNA is shown for RNA quality. Light microscope photographs of the cell morphology of OV-90, OV-90:EV[2], OV-90:EV[9], OV-90:*CCL2*[23] and OV-90:*CCL2*[49], arrows indicate representative cell morphology (**c**). Light microscope photographs are × 100 magnification. Cell viability by XTT assay of OV-90, OV-90:EV[2], OV-90:EV[9], OV-90:*CCL2*[23] and OV-90:*CCL2*[49], representative results from one independent experiment that was performed in triplicate (**d**). Cell viability was measured over 8 days and cell culture media-only wells served as controls (OSE and OSE-G418).

relative to the OV-90 cell line was lower, as measured using the XTT cell viability and proliferation assay, these differences were not significant (Figure 1d).

OV-90 is able to form spheroids in hanging drop cultures,[29,32] and so were the *CCL2*-expressing clones (Figure 2a). Both of the EV clones appeared to have lost this capacity though they maintained the ability to form numerous small cell aggregates (Figure 2a). This phenotype was observed with five other independently selected EV clones (data not shown).

OV-90 is able to form large colonies in cell culture.[29] The *CCL2*-expressing clones formed fewer colonies as compared with OV-90 and the EV clones, though this difference was not significant (Figures 2b–d). Also, the colonies formed by the *CCL2*-expressing clones appeared to be smaller than those formed by OV-90 and the EV clones (Figures 2b and c).

The effect of overexpressing *CCL2* on cell migration was assayed using *in vitro* 'wound healing' assays. There appeared to be modest differences in the rate at which cells migrated within the
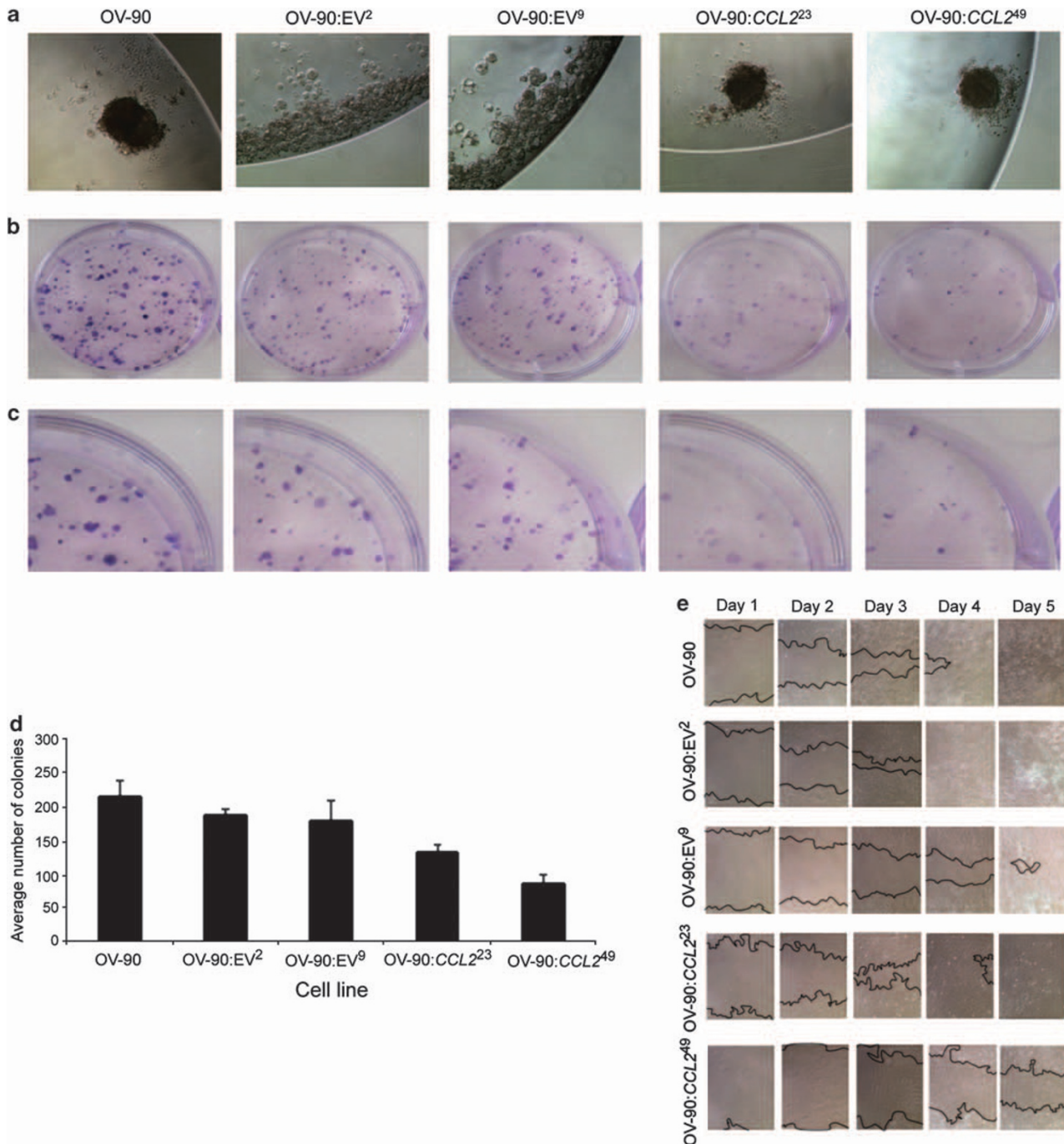

Figure 2. *In vitro* characterization of the *CCL2*-expressing clones. Light microscope photographs of OV-90, OV-90:EV[2], OV-90:EV[9], OV-90:CCL2[23] and OV-90:CCL2[49] spheroids on day 8 of the assay, edges of the hanging droplets are shown (**a**). Colony forming ability of OV-90, OV-90:EV[2], OV-90:EV[9], OV-90:CCL2[23] and OV-90:CCL2[49] (**b**). Magnified ($\times$4) colonies formed by OV-90, OV-90:EV[2], OV-90:EV[9], OV-90:CCL2[23] and OV-90:CCL2[49] (**c**). Average number of colonies formed in colony formation assay, representative results from one independent experiment that was performed in triplicate (**d**). Wound healing assay of OV-90, OV-90:EV[2], OV-90:EV[9], OV-90:CCL2[23] and OV-90:CCL2[49] over a period of 5 days (**e**). Light microscope photographs are $\times$100 magnification.

wound, particularly with clone OV-90:*CCL2*[49] (Figure 2e). By day 5, OV-90 and all clones, with the exception of clone OV-90:*CCL2*[49], filled the wound. Clone OV-90:*CCL2*[49] filled the wound by day 7.

Tumourigenicity assays of *CCL2*-expressing clones

OV-90 cells are able to form tumours when injected at both subcutaneous (s.c.) and intraperitoneal (i.p.) sites in immunocompromised mice, where there is also an accumulation of ascites at the i.p. site.[31] Using severe combined immunodeficiency mice, the *CCL2*-expressing clones were tumourigenic at the s.c. site, where there were no significant differences in the time-to-kill, final mean tumour volume or mean tumour growth rate as compared with OV-90 (Figure 3, Supplementary Table S2). Although the *CCL2*-expressing clones were also tumourigenic at the i.p. site, the survival, as measured by the days-to-kill, was significantly longer
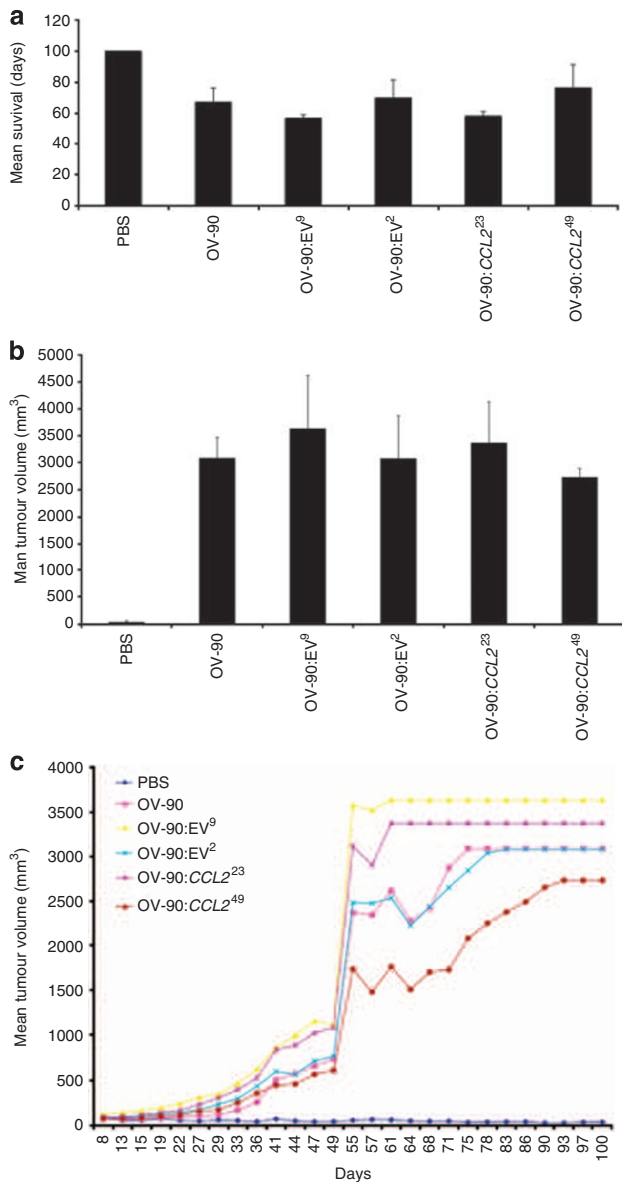
for each *CCL2*-expressing clone when compared with OV-90 and both of the EV clones ($P < 0.00853$ and $P < 0.001$, by t-test and Kaplan–Meier survival curve analyses, respectively; Figure 4, Supplementary Table S2). In addition to analysing all groups in the Kaplan–Meier survival curve analyses, all possible individual pairs of groups were also analysed and resulted in significant differences in survival between each *CCL2*-expressing clone and OV-90 or either of the EV clones ($P \leqslant 0.001$; Supplementary Figure S1). Using primer-specific RT–PCR assays vector-driven *CCL2* expression was detected in the xenografts derived from *CCL2*-expressing clones (Figure 5a). There were no overt differences in the appearance or presentation of the tumours, though some of the tumours from the *CCL2* clone-injected mice were less bloody than those of OV-90-injected mice (Supplementary Table S2). Xenografts derived from OV-90 and both *CCL2*-expressing clones, from both the i.p. and s.c. experiments, were indistinguishable when hematoxylin and eosin slides were examined by a gynecologic pathologist. All xenografts appeared as high-grade serous tumours, and displayed high levels of mitosis and necrosis, with no overt differences in terms of infiltrating cells (Figure 5b). Although all of the OV-90-injected mice showed evidence of tumour implants on either the peritoneum or the abdominal organs, this was not observed in all of the *CCL2* clone-injected mice (Supplementary Table S2). However, the sample size was small and the experiments were not designed to quantitatively measure these features.
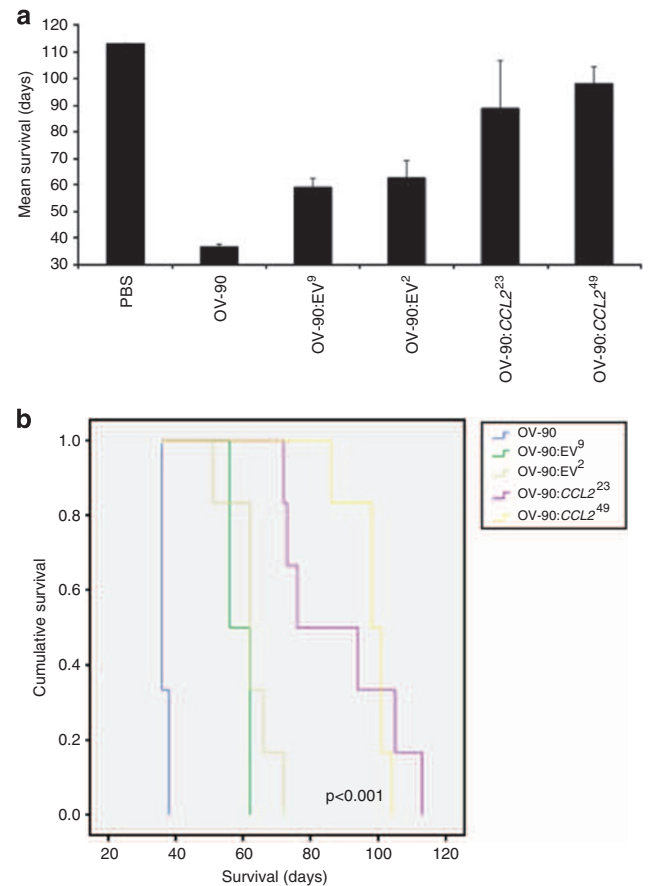

Figure 3. S.c. injection site *in vivo* tumourigenicity assay. Mean survival, in days, of mice injected with OV-90, OV-90:EV[2], OV-90:EV[9], OV-90:*CCL2*[23] or OV-90:*CCL2*[49] at s.c. injection sites with six mice per group, and four phosphate-buffered saline (PBS)-injected mice as injection controls (**a**). Final mean tumour volume per group (**b**). Mean tumour volume per group over time (**c**).

Figure 4. I.p. injection site *in vivo* tumourigenicity assay. Mean survival, in days, of mice injected with OV-90, OV-90:EV[2], OV-90:EV[9], OV-90:*CCL2*[23] or OV-90:*CCL2*[49] at i.p. injection sites with six mice per group, and four PBS-injected mice as injection controls (**a**). Kaplan–Meier survival curves comparing all groups (**b**).
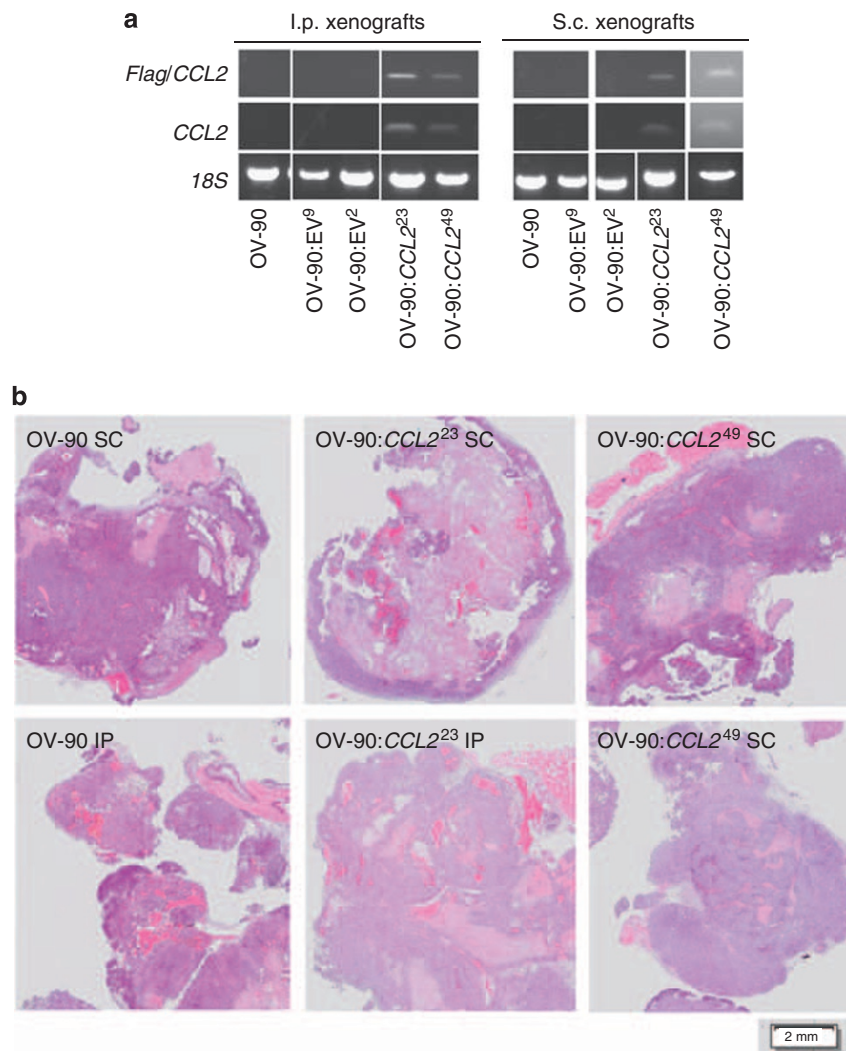
Figure 5. *CCL2* expression and hematoxylin and eosin staining of xenografts. Semi-quantitative RT–PCR analysis of endogenous *CCL2* (*CCL2*) and introduced, expression vector-derived, *CCL2* (*Flag/CCL2*) performed on cDNA samples prepared from a subset of xenografts obtained from both i.p. and s.c. injection sites (**a**). The expression of 18S cDNA is shown for RNA quality. Hematoxylin and eosin staining of OV-90, OV-90:*CCL2*[23] and OV-90:*CCL2*[49] xenografts obtained from both s.c. and i.p. injection sites at time of killing (**b**). Images were obtained from the OlyVIA image viewer (Olympus America Inc., Center Valley, PA, USA).

Expression microarray analysis of *CCL2*-expressing clones

A transcriptome analysis was performed on RNA extracted from the OV-90 and *CCL2*-expressing clone cell lines. The gene expression profiles were highly correlated (>0.93), suggesting that modest differences in their transcriptomes occurred. Two-way comparative analyses were performed comparing OV-90 and the *CCL2*-expressing clones to determine whether biological networks characteristic of EOC were affected in these clones. Based on defined criteria to reduce biases owing to technical noise,[33] 67 genes were identified as differentially expressed in the *CCL2*-expressing clones (Table 1). These genes were significantly enriched for gene ontology terms such as immune response and defence response (Figure 6a). Ingenuity pathway analysis found cancer and immune cell trafficking to be significantly enriched biological functions, and identified 'cell-to-cell signalling and interaction/inflammatory response/cellular movement' to be the top network (Figure 6b). A survey of the literature found 46% (*n* = 31) of these genes associated with EOC research (Table 1).

CCL2 gene and protein expression in HGOSC, and relationship with overall and disease-free survival

Using a custom-made gene expression platform,[34] we evaluated *CCL2* expression in 79 HGOSC samples. About 65% of these HGOSCs (*n* = 51) exhibited *CCL2* expression at levels lower than that observed in whole ovary (Figure 7a). In whole ovary, stromal cells predominate and only a small proportion represent the single layer of surface epithelial cells, which is one of cell types proposed to be the origins of EOC.[35–37] Relative to the mean or median of the expression of the NOSEs, *CCL2* was significantly (*P* = 0.015) underexpressed in 100% (*n* = 79) and 98.7% (*n* = 78) of the HGOSCs, respectively.

We also investigated CCL2 protein expression by immunohistochemistry using a tissue array that contained cores from 65 of the above HGOSC samples. The majority of cores (77%) exhibited no detectable immunostaining (40%) or detectable, but low, levels of staining (37%; Figure 7b, Table 2). Moderate or clearly detectable staining was observed in 23% of samples, where the staining pattern was not always uniform across the epithelial cell

Table 1. Genes differentially expressed at least threefold in both *CCL2*-expressing clones relative to OV-90

Probe set	Cytoband	Gene	OV-90 expression value	OV-90:CCL2[49] fold change	OV-90:CCL2[23] fold change	
216598_s_at	17q12	CCL2	5.0	409.4	155.7	<
222227_at	18q23	ZNF236	5.2	402.7	526.6	
207086_x_at	Xp11.23	GAGE5	5.5	27.9	641.5	
215101_s_at	4q13.3	CXCL5	33.9	25.2	24.2	<
227238_at	11p14.3	MUC15	13.6	22.6	18.5	
232010_at	4q32.3	FSTL5	5.2	22.2	21.1	
220062_s_at	Xq27	MAGEC2	37.9	16.6	4.1	
207739_s_at	Xp11.23	GAGE1	10.9	15.5	403.8	<
211403_x_at	Xp22.32	VCX2	30.3	15.1	16.7	
231265_at	4p12	COX7B2	29.5	13.7	18.1	
228697_at	6q22.32	HINT3	37.3	11.0	16.7	
206336_at	4q21	CXCL6	98.3	10.0	28.1	
216471_x_at	Xp11.22	SSX2	35.9	8.1	27.5	<
204446_s_at	10q11.2	ALOX5	17.1	7.9	9.4	<
213317_at	6p12.3	CLIC5	19.1	7.5	7.5	
206626_x_at	Xp11.23	SSX1	45.2	6.5	23.9	<
241879_at	3q28	LPP	31.8	6.4	5.6	<
207666_x_at	Xp11.23	SSX3	26.8	6.3	26.6	
225275_at	5q14	EDIL3	36.0	6.2	80.8	
229070_at	6p24.1	C6orf105	39.9	6.0	6.8	
202902_s_at	1q21	CTSS	20.8	5.9	10.2	<
230788_at	6p24.2	GCNT2	49.2	5.6	4.1	
1554696_s_at	18p11.32	TYMS	84.1	5.4	6.2	
205381_at	7q22.1	LRRC17	138.4	5.3	24.9	
222712_s_at	3q21.2	MUC13	31.1	5.0	9.7	<
1554768_a_at	4q27	MAD2L1	118.0	5.0	3.3	<
211506_s_at	4q13–q21	IL8	81.1	4.7	10.6	<
1559316_at	5p14.3	AK093362	27.0	4.7	5.7	
229349_at	6q21	LIN28B	34.7	4.2	3.9	<
204470_at	4q21	CXCL1	486.6	4.1	3.9	<
201858_s_at	10q22.1	SRGN	59.7	4.0	14.1	
206662_at	5q14	GLRX	74.9	3.8	3.5	
221477_s_at	6q25.3	SOD2	41.8	3.7	4.5	<
212185_x_at	16q13	MT2A	226.9	3.7	5.3	<
213872_at	6p22.3	C6orf62	89.7	3.7	3.9	
208581_x_at	16q13	MT1X	165.4	3.7	4.7	
216336_x_at	16q13	MT1E	97.9	3.6	3.4	
225647_s_at	11q14.2	CTSC	111.8	3.5	3.1	<
206461_x_at	16q13	MT1H	111.4	3.4	3.9	
1555814_a_at	3p21.3	RHOA	179.2	3.3	3.3	<
210950_s_at	8p23.1–p22	FDFT1	154.5	3.3	3.2	
214079_at	14q11.2	DHRS2	56.7	3.2	54.3	<
200665_s_at	5q31.3–q32	SPARC	86.9	3.2	15.7	<
201627_s_at	7q36	INSIG1	99.9	3.0	8.1	
205226_at	8p22–p21.3	PDGFRL	62.4	3.0	6.4	
203159_at	2q32–q34	GLS	241.0	−3.3	−3.9	
210076_x_at	1p31	SERBP1	231.4	−3.4	−3.6	<
232165_at	8q24.3	EPPK1	477.8	−3.5	−4.5	
219301_s_at	7q35	CNTNAP2	139.6	−3.6	−13.6	<
235048_at	5q13.3	FAM169A	241.2	−3.7	−8.7	
240385_at	18q11.2	GATA6	293.8	−4.1	−12.6	<
200768_s_at	2p11.2	MAT2A	2351.0	−4.2	−5.4	
241137_at	6p21.33	DPCR1	710.1	−4.3	−28.0	
204818_at	16q24.1–q24.2	HSD17B2	1346.5	−4.5	−4.5	<
204450_x_at	11q23–q24	APOA1	158.6	−4.5	−7.1	<
236313_at	9p21	CDKN2B	305.8	−4.7	−3.4	<
228846_at	2p13–p12	MXD1	262.7	−4.9	−8.9	<
201963_at	4q35	ACSL1	154.7	−6.2	−10.6	
210319_x_at	5q35.2	MSX2	232.5	−6.3	−3.4	<
202935_s_at	17q23	SOX9	159.9	−6.3	−3.2	<
228461_at	2q13	SH3RF3	256.1	−6.5	−3.7	
213967_at	8q21.2	RALYL	160.7	−7.4	−32.1	
231270_at	8q21.2	CA13	295.5	−7.6	−11.9	
212295_s_at	13q12–q14	SLC7A1	1443.0	−15.7	−4.4	
205975_s_at	2q31.1	HOXD1	204.5	−17.3	−9.0	<
231385_at	12p13.31	DPPA3	146.3	−29.3	−29.3	
1552767_a_at	Xq26.2	HS6ST2	221.1	−44.2	−27.6	<

<, Genes have been previously reported in an ovarian cancer context. Fold change in gene expression highlighted in red for overexpression and green for underexpression relative to OV-90 cell line.
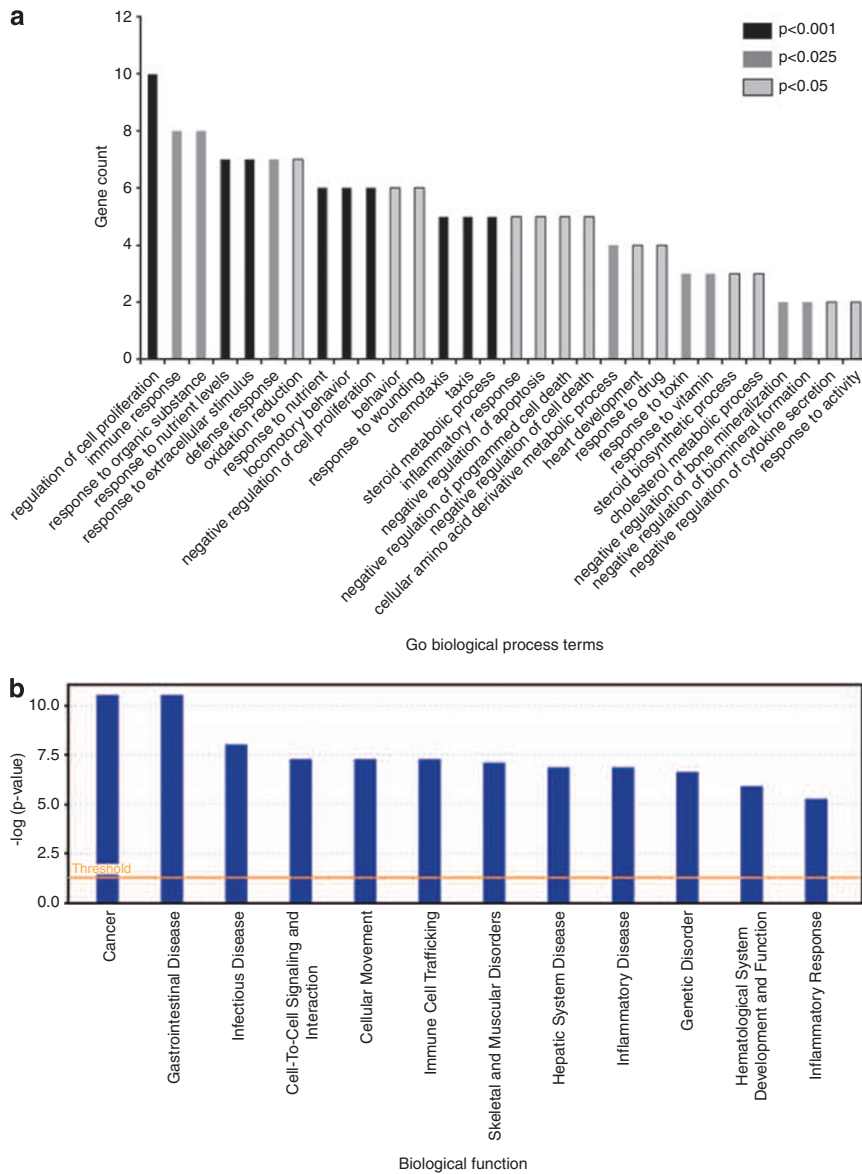
a

b

Figure 6. Enriched biological term and biological function analysis of the 89 probe sets differentially expressed in the *CCL2*-expressing clones. Significantly enriched GO biological process terms derived from the DAVID functional annotation classification tool, with *P*-values < 0.05 classified as significant by a modified Fisher's exact test (**a**). Ingenuity pathway analysis of enriched biological functions (**b**).

components of the tumour (Figure 7b). Immunohistochemistry analysis was also evaluated in an additional 122 HGOSC samples, which were included in the same array as described above. The same staining patterns were observed, where the majority of cores (71%) exhibited no detectable immunostaining (42%) or detectable, but low, levels of staining (29%; Table 2).

Although no cores were available from whole ovary with intact NOSEs, the tissue array contained cores from 11 normal fallopian tube samples, which is a recently posited origin of some HGOSCs.[38] Interestingly, CCL2 staining was uniform and particularly evident in the fallopian tube epithelial cells (Figure 7b).

Clinical data to assess overall and disease-free survival were available for the 187 cases examined for CCL2 immunostaining. The relationship between CCL2 immunostaining and overall or disease-free survival was evaluated using Kaplan–Meier survival curve analyses. The comparison of cases whose tumours exhibited negative or low CCL2 staining (*n* = 136) to those whose tumours

exhibited moderately or clearly detectable CCL2 staining (*n* = 51) found no significant relationship between CCL2 protein expression and either overall or disease-free survival in this sample set (Figures 7c and d). The analyses were performed using all possible combinations based on staining patterns grouped according to absent, low, moderate and high staining levels and no significant relationship was observed with overall or disease-free survival for any of these comparative groups.

DISCUSSION

Ectopically overexpressing *CCL2* in the OV-90 EOC cell line significantly affected the tumourigenic potential in a mouse xenograft model at i.p. but not s.c. sites. The overexpressing clones differed from the OV-90 parental cell line in their cell morphology and they were less viable. They also exhibited a reduced capacity to form large colonies in colony formation assays, and exhibited a
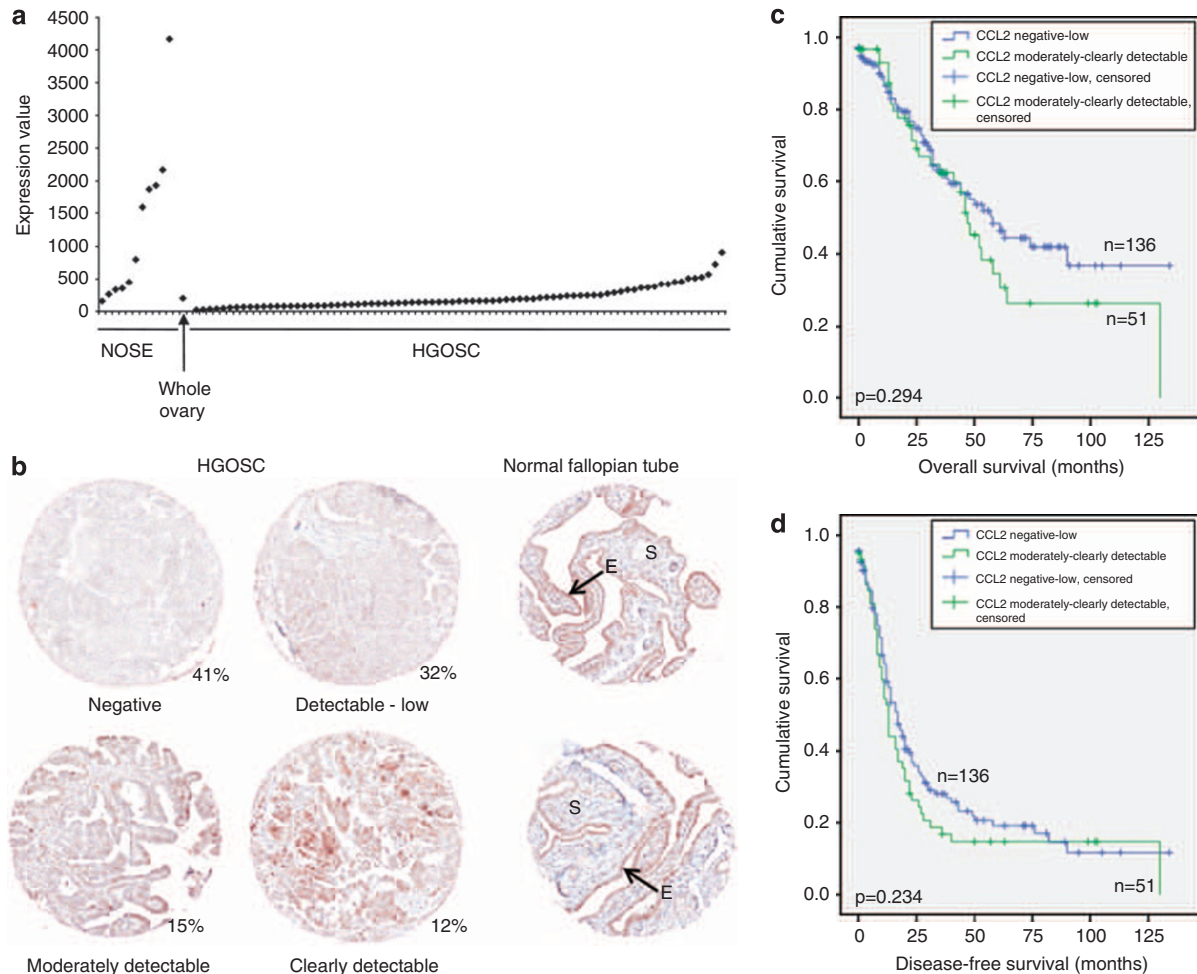
Figure 7. *CCL2* expression in HGOSC. *CCL2* expression in 11 NOSE samples, normal whole ovary and 79 HGOSC samples as determined by Ziplex Research System expression array (Axela Inc., Toronto, Ontario, Canada) (**a**). Examples of CCL2 expression in cores from four HGOSC samples (left panel) showing, negative, detectable but low, moderately detectable and clearly detectable CCL2 staining, and examples of CCL2 staining in cores from two normal fallopian tube tissue samples (right panel) (**b**). Percentages refer to the proportion of the 187 HGOSC samples showing negative, detectable but low, moderately detectable and clearly detectable staining patterns of protein expression (Table 2). 'E' indicates epithelial cells and 'S' indicates stromal cells. Immunohistochemistry images were obtained from the OlyVIA image viewer (Olympus America Inc.). The Kaplan–Meier survival curve analysis of HGOSC cases for overall (**c**) and disease-free (**d**) survival (in months) of patients whose tumours showed negative or low CCL2 staining ($n = 136$) compared with patients whose tumours showed moderately or clearly detectable CCL2 staining ($n = 51$). Indicated *P*-values were derived from log-rank tests.

modest effect on cell migration in wound healing assays. These results suggest the possibility that overexpressing *CCL2* altered the growth characteristics of OV-90, although these differences were not significant. The modest alterations of the growth characteristics observed in *in vitro* assays could explain the latency in tumour formation and significantly increased survival observed in mouse xenograft assays at i.p. sites. It does not explain the observation that tumours from the *CCL2*-expressing clones formed at s.c. sites at the same rate as OV-90. A similar observation was made by Nokihara *et al.*[39] that reported that mice injected intravenously with *CCL2*-expressing transfectant clones of a human lung adenocarcinoma cell line survived longer and exhibited a delay in metastasis formation, whereas no difference, relative to controls was observed in mice injected at s.c. sites. The authors proposed an NK cell-dependent mechanism where the anti-tumour effects by cytokines are regulated differently by various organ microenvironments.[39] Furthermore, dendritic cell distributions and plasma levels of angiogenic cytokines in response to tumour cell injections have been shown to be different depending on whether the cells were

injected s.c. or i.p.[40,41] In addition, our research group has previously reported that OV-90-derived xenografts from s.c. injection sites had a different expression profile when compared with xenografts from i.p. injection sites, suggesting that the microenvironment in which the cells are injected impacts their transcriptome.[29,32] Collectively, these results indicate that the s.c. and i.p. microenvironments differ in responses to tumour cell injections, although the specific differences have not been fully elucidated. For ovarian cancer, the i.p. injection site is a better model, as it is more reflective of the human condition.

Gene expression microarray analysis revealed that immune response-related genes and pathways were differentially expressed in the *CCL2*-expressing clones, relative to OV-90. The upregulated genes included tumour antigens, such as those encoded by the *MAGE* and *GAGE* genes, which have been shown to induce tumour-specific immune responses (reviewed in Bodey[42]). The expression of such genes along with *CCL2* may have contributed to the latency in tumour formation at i.p. sites in our study by inducing an anti-tumour response. This notion is supported by the observation that a CCL2-expressing lung

Table 2. Summary of immunohistochemistry analysis of CCL2 in HGOSC samples

	HGSOC cohort (n)		
	Initial HGOSC cohort (65)	Additional HGOSC samples (122)	All HGOSC samples (187)
Staining pattern (n (%))			
Negative	26 (40)	51 (42)	77 (41)
Detectable but low	24 (37)	35 (29)	59 (32)
Moderately detectable	9 (14)	19 (16)	28 (15)
Clearly detectable	6 (9)	17 (14)	23 (12)

Abbreviation: HGSOC, high-grade ovarian serous carcinomas.

adenocarcinoma cell line contributed to an NK cell-dependent anti-tumour response, as mentioned above.[39] In addition, a recent study involving mice injected with the 4T1 mouse breast cancer cell line resulted in an accumulation of neutrophils exhibiting cytotoxic effects to tumour cells in the pre-metastatic lung.[43] The cytotoxic activity was attributed to the secretion of CCL2.[43] Thus, NK cells and neutrophils may be involved in anti-tumour activities as a consequence of CCL2 expression. Both of these cell types are present in severe combined immunodeficiency mice (used in this study) that despite lacking adaptive immune components have intact innate immune components, including NK cells and neutrophils. Interestingly, four known chemoattractants for neutrophils (*CXCL1*, *CXCL5*, *CXCL6* and *IL8*)[44] were among the genes found overexpressed in the *CCL2*-expressing clones, suggesting the possibility that neutrophils may have contributed to tumour latency in our study.

In another recent study, hepatocellular carcinoma patients exhibiting high CCL2 expression, along with other chemokines, had better survival than those that did not, and this effect was only observed in patients with early-stage disease.[45] A role for CCL2 in early stages of tumour development was also suggested in the study by Granot *et al*.,[43,45–47] which suggested that CCL2 expression levels may be critical in maintaining an anti-tumour environment, but that the tumour cells may, under certain circumstances, outcompete the cytotoxic effects of immune cells, escaping anti-tumour responses, resulting in clinically detectable tumours and/or disease with poorer outcomes. This may explain why the xenografts derived from OV-90 and the *CCL2*-expressing clones appeared indistinguishable when they were collected from the mice at killing.

The *CCL2*-expressing clones also showed upregulation of genes previously implicated in EOC, such as the TSG *SPARC*,[48] suggesting that some of the transcriptional changes may be relevant to EOC biology. Based on our transcriptome analysis OV-90 does not appear to express the canonical receptor for CCL2, *CCR2b*[49] nor *CCR1*, another proposed CCL2 receptor,[50] and neither of these receptors were differentially expressed in our comparative analyses (data not shown). Thus, the transcriptional changes observed in the *CCL2*-expressing clones may be due to signalling through a yet unidentified CCL2 receptor as other studies have also shown CCL2 mediated signalling in the absence of *CCR2*.[51,52]

We have reaffirmed that *CCL2* gene expression[19] is significantly underexpressed or absent in HGOSC and that this is consistent with protein expression. CCL2 expression in the epithelial cells of the fallopian tube is intriguing in light of the recent hypothesis that these cells, in addition to NOSE cells, are the progenitor cell type for HGOSC.[38] Our immunohistochemistry results are consistent with earlier findings, which demonstrated CCL2

secretion by normal fallopian tube epithelial cells.[53] It was proposed that chemokines, including CCL2, expressed by the epithelial cells of the female reproductive tract contribute to normal physiological homoeostasis and protection from pathogens by activating immune cells.[53] In addition to this protective function, chemokines, such as CCL2, may protect these cells from malignant transformation, again suggesting that *CCL2* may be involved early in tumour development.

Our gene expression results are consistent with recently reported gene expression data extracted from a large independent study that applied a different gene expression platform by the Cancer Genome Atlas Research Network (TCGA).[54] *CCL2* was found underexpressed at least twofold, relative to normal fallopian tube samples, in about 68% of the 506 HGOSCs, where only 8% of samples exhibited a greater than twofold difference in gene expression. As our immunohistochemistry results indicate clearly detectable CCL2 protein expression in the epithelial cell component of the fallopian tubes and less so in the stromal cell component, it is possible that this independent comparative analysis is an underrepresentation of the gene expression pattern of *CCL2* in HGOSC samples.

A transcriptional signature predictive of overall survival was identified using a subset of gene expression data and 215 HGOSCs in the report by the TCGA, and *CCL2* was not among the genes identified, consistent with our findings.[54] The TCGA study also reported that four robust expression subtypes exist in HGOSC, however, the genes making up these subtypes were not reported.[54] It would be interesting to see whether *CCL2* contributed to one of these subtypes. It would also be interesting to re-evaluate associations with overall survival when protein expression is taken into consideration in the TCGA samples as well as the expression subtypes. These results (including our own) are in part in contrast to the findings of Fader *et al*.[24] where *CCL2* expression was found significantly higher in chemosensitive versus chemoresistant tumours and gene expression was correlated with progression-free survival. That study used *CCL2* expression microarray data from a small set of 37 serous EOC samples, and defined expression groups using a partitioning algorithm that identified an optimal threshold value of expression for chemosensitivity.[24] These differences in methodology, such as using a well-defined cohort to establish a threshold of expression, may explain why we found no association between CCL2 protein expression and patient outcome. Thus, while underexpression is a consistent feature of the majority of HGOSC samples based on both gene and protein expression analyses further research, using clinically well-defined cohorts and an appropriate expression threshold, is required to resolve possible associations with disease outcomes.

In summary, *CCL2* is underexpressed in the majority of HGOSCs, and transfection of this gene into the EOC cell line OV-90 resulted in prolonged survival and delayed tumour formation *in vivo*. To our knowledge this is the first investigation of the effects of *CCL2* expression on the tumourigenicity of an EOC cell line. Given the known chemoattractant properties of *CCL2*, its overexpression may have modified tumourigenicity by inducing an anti-tumour immune response. Future studies are warranted to elucidate the mechanism by which *CCL2* expression contributed to tumour latency, as well as to gain a better understanding of the earliest events of EOC tumourigenesis.

MATERIALS AND METHODS

Tissue specimens

The HGOSC and normal tissue samples were collected with informed consent from patients undergoing surgeries performed at the Centre hospitalier de l'Université de Montréal—Hôpital Notre-Dame as described (Supplementary Table S3).[2,55] Clinical features, such as disease stage, and tumour characteristics, such as grade and histopathological subtype, were assigned by a gynaecologic-oncologist and/or gynaecologic-pathologist

according to the criteria established by the International Federation of Gynaecology and Obstetrics. Disease-free survival, defined as time to doubling of the upper normal limit of the serum cancer antigen marker CA-125 or the detection of a new lesion by ultrasound or CT scan imaging, and overall survival, defined according to the Response Evaluation Criteria in Solid Tumours[56] were extracted from the Système d'Archivage des Données en Oncologie.

Cell lines
The EOC cell line OV-90 was derived from the ascites of a stage IIIc/grade 3 adenocarcinoma from a chemotherapy naïve patient, as described.[31] The non-tumourigenic Chr3 transfer radiation hybrid RH-6 was derived by fusing a neomycin clone of OV-90 (OV-90 neo[r]), and an irradiated B78MC166 mouse cell line containing human Chr3 as described previously.[29] The cell lines were cultured in Ovarian Surface Epithlelium (OSE) medium (consisting of 50:50 medium 199:105 (Sigma-Aldrich, St Louis, MO, USA)) supplemented with 2.5 μg/ml amphotericin B, 50 μg/ml gentamicin and 10% fetal bovine serum as described previously.[31,57] The primary cultures of NOSE samples were described previously.[19,55,58]

Nucleic acid extraction
Total RNA was extracted with TRIzol reagent (Gibco/BRL, Life Technologies Inc., Grand Island, NY, USA) from the cell lines or primary cultures of NOSEs grown to 80% confluency in 100 mm Petri dishes as described previously.[19,29,55,58,59] RNA was extracted from flash-frozen HGOSC tumours or tumour xenografts using the RNeasy Plus Mini Kit (Qiagen, Mississauga, Ontario, Canada) according to the kit instructions. Tissues were homogenized, using a 20-gauge (1.5 inch) needle and syringe. RNA quality was assessed by gel electrophoresis and 2100 Bioanalyzer analysis using the Agilent RNA 6000 Nano kit (Agilent Technologies, Waldbronn, Germany).

CCL2 expression in HGOSC samples
CCL2 expression was assessed using a custom Ziplex Research System gene expression array platform (Axela Inc.), which contained probes for *CCL2* and other genes as described in detail elsewhere.[34] RNA from whole ovary (Stratagene, La Jolla, CA, USA) was used as reference for comparison.

Immunohistochemistry
CCL2 protein expression was assessed by immunohistochemistry. A tissue array containing 0.6 mm cores was constructed from paraffin-embedded tissue blocks selected based on a review of hematoxylin and eosin-stained slides of HGOSC and normal fallopian tube samples. The cores were arrayed 1 mm apart onto a single paraffin block. The tissue array contained tissue cores that represented 65 HGOSCs also investigated for gene expression, 11 normal fallopian tube samples and 122 additional HGOSCs. Immunohistochemistry analysis was performed using 5-μm sections mounted onto frosted plus slides. Staining was performed with an antibody against human CCL2 (1:100; R&D Systems, Burlington, Ontario, Canada), using the Ventana Benchmark XT system (Ventana Medical Systems, Inc., Tucson, Arizona). The tissue array was scanned and images viewed using the Olympus OlyVIA software 2.3 (Build 8529, Olympus America Inc.). Two observers examined the images and independently scored the staining intensity of the epithelial cells in each core as absent (negative), low (detectable but low), moderate (moderately detectable) or high (clearly detectable). The inter-observer correlation coefficient for CCL2 protein expression (0.896) was calculated using the SPSS software version 16.0 (SPSS Inc., Chicago, IL, USA), where the minimum threshold was 0.7.

Generation of CCL2 clones
CCL2-expressing clones were generated by transfecting OV-90 cells with the commercially available pDream2.1 vector containing the full coding sequence of *CCL2* in frame with the Flag tag sequence or empty pDream2.1 vector (GeneScript, Piscataway, NJ, USA). The insert was DNA sequence-verified at the McGill University and Genome Quebec Innovation Centre (http://www.gqinnovationcenter.com/). Transfection was carried out using lipofectamine 2000 and Opti-MEM (both from Invitrogen, Burlington, Ontario, Canada). The *CCL2*-expressing and EV clones were selected and maintained in the presence of 800 and 400 μg/ml, respectively, of Geneticin (Life technologies inc., Burlington, Ontario, Canada) in OSE complete medium as described above.[55] CCL2 protein expression was assessed by ELISA using the Quantikine Human CCL2/MCP-

1 kit (R&D Systems) according the manufacturer's protocol. Briefly 600 000 cells were plated in each of a six-well plate, after 24 h the media was replenished, and after a further 40 h the supernatant was removed, filtered (28 mm syringe filter, Corning, Lowell, MA, USA) and used in the enzyme-linked immunosorbent assay. *CCL2* expression was tested by RT–PCR as described below. Forty-seven stable *CCL2* clones were isolated, and two *CCL2* clones (OV-90:*CCL2*[23] and OV-90:*CCL2*[49]) expressing the highest levels of CCL2 by enzyme-linked immunosorbent assay, were selected for further analyses. Sixteen EV clones were generated and 2 (OV-90:EV[2] and OV-90:EV[9]) were randomly selected for further analyses.

RT–PCR analyses
RT–PCR analysis was performed using cDNA synthesized as described.[29,60] Primers were designed using the Primer3 software[61] based on reference sequence *NM_002982*, and on the genomic structure of the *CCL2*,[62] as well as the vector sequence. Endogenous *CCL2* expression was detected using 5'-tcagccagatgcaatcaatg-3' forward primer and 5'-tggaatcctgaacccacttc-3' reverse primer, yielding a 191-base pair product. Vector-driven *CCL2* expression was detected using the same forward primer and 5'-cttatcgtcgtcatccttgta-3' as the reverse primer, yielding a 280-base pair product. The RT–PCR-based assays and visualization of products were performed essentially as previously described.[63]

XTT cell viability assay
Cell viability was determined by an XTT-based *in vitro* toxicology assay kit according to the manufacturer's protocol (Sigma-Aldrich, Oakville, Ontario, Canada). In total, 4000 cells per well were seeded, in triplicate, in a 96-well plate, and separate plates were used for each time point (day) of the assay. Changes in optical density, a read-out for cell viability, were monitored over 8 days. The assay was repeated three times.

Spheroid growth
OV-90 and the clones were tested for their capacity to form spheroids in hanging drop culture, as described.[64] Spheroid formation was monitored by light microscopy over 8 days.[32] The assay was preformed in triplicate.

Colony formation
The ability of the cells to form colonies was assessed by colony formation assays. In all, 500 cells suspended in OSE complete medium were seeded, per well, in a six-well plate, in triplicate, and allowed to grow for a period of about 2 weeks, at which time media was removed, cells washed with 1X phosphate-buffered saline and fixed in methanol. Post-fixation, the cells were stained with Giemsa stain, modified solution overnight (Sigma-Aldrich). Colonies were counted, and the mean of the triplicates calculated. The assay was repeated four times.

Wound healing assay
The ability of OV-90 and the clones to migrate and fill a wound was determined using Culture-Inserts (Ibidi, Ingersoll, Ontario, Canada), according to the manufacturer's protocol. Briefly, 50 000 cells were seeded into the outer wells of two adjacently placed Culture-Inserts in a volume of 70 μl and incubated at 37 °C. Once the wells reached confluence, the Culture-Inserts were removed creating a 1-mm gap (wound). Cell migration was then monitored until the gap was filled. The assay was repeated twice, in triplicate.

In vivo tumourigenicity assays
Tumourigenic potential was assessed based on the ability to form tumours in 42-day-old female severe combined immunodeficiency mice (severe combined immunodeficiency CB17, Charles River, Wilmington, MA, USA) at s.c. left gluteal (*n* = 6 mice) and i.p. injection sites (*n* = 6 mice). Each mouse was injected at either site with 1 × 10^{6} of OV-90, OV-90:*CCL2*[23], OV-90:*CCL2*[49], OV-90:EV[2] or OV-90:EV[9] cells suspended in phosphate-buffered saline for the i.p. site and 50% matrigel (BD Biosciences, Mississauga, Ontario, Canada) for the s.c. site experiment. Animals were housed under sterile conditions in a laminar flow environment with *ad libitum* access to food and water. Tumour formation was measured over 113 days. Animals were killed and tumours collected before neoplastic masses reached >2500 mm[3] in the s.c. experiment, or maximal tumour burden and ascites formation in the i.p. experiment, according to the guidelines of the Canadian Council on Animal Care. Phosphate-buffered saline-injected mice (*n* = 4) served as injection controls in each experiment. Mice were

monitored twice weekly and data were collected for mouse weight (i.p. and s.c. experiments) and tumour volume (s.c. experiments).

Expression microarray analysis of *CCL2* clones

Microarray expression analysis of total RNA from OV-90:*CCL2*[23], OV-90:*CCL2*[49] and OV-90 cell lines was performed once per sample using the Affymetrix GeneChip U133 Plus 2 array (Affymetrix, Santa Clara, CA, USA) at the McGill University and Genome Quebec Innovation Centre (http://gqinnovationcenter.com). Gene expression levels were determined from scanned images using the MAS5.0 software (Affymetrix Microarray Suite). To eliminate systematic biases when comparing the expression values from independently generated data sets, the raw data were normalized and rescaled as previously described.[29,59,65,66] Differentially expressed genes were defined as those that exhibited at least a threefold difference in expression in both *CCL2* clones (same pattern), relative to OV-90, and had an expression value difference of at least 100 in both *CCL2* clones relative to OV-90.

Statistical analyses and bioinformatic analyses

An independent sample *t*-test, not assuming equal variance, was performed to determine the significance of *CCL2* expression using the SPSS software (Statistical Product and Service Solution Package). Student's *t*-tests were performed to identify significant differences in *in vitro* and *in vivo* analyses using Simple Interactive Statistical Analysis (http://www.quantitativeskills.com/sisa/). Kaplan–Meier survival curve analysis coupled with the log-rank test was performed to evaluate survival in mouse tumourigenicity assays using the SPSS software. Survival curve analysis was performed on all groups combined (Figure 4b) as well as on all possible pairs of groups (Supplementary Figure S1). The relationship between CCL2 immunostaining (using all possible groupings based on absent, low, moderate and high staining levels) and overall or disease-free survival as defined above were evaluated using Kaplan–Meier survival curve analyses coupled to the Mantel–Cox log-rank test, and performed using the SPSS software. *P*-values <0.05 were considered significant.

The 89 probe sets (67 genes) found differentially expressed at least threefold in both *CCL2* clones relative to OV-90 were evaluated by the DAVID Bioinformatics Resources 6.7 functional annotation clustering tool.[67] Significant GO biological process terms were extracted along with gene counts and *P*-values as determined by a modified Fisher's exact test. The associated biological functions of these probe sets were also evaluated using Ingenuity Pathways Analysis (Ingenuity Systems, www.ingenuity.com). Right-tailed Fisher's exact test was used to calculate a *P*-value determining the probability that each biological function assigned to that data set is due to chance.

CONFLICT OF INTEREST

The authors declare no conflict of interest.

REFERENCES

1 Liu Y, Ganesan TS. Tumour suppressor genes in sporadic epithelial ovarian cancer. *Reproduction* 2002; **123**: 341–353.

2 Dion F, Mes-Masson AM, Seymour RJ, Provencher D, Tonin PN. Allelotyping defines minimal imbalance at chromosomal region 17q25 in non-serous epithelial ovarian cancers. *Oncogene* 2000; **19**: 1466–1472.

3 Foulkes WD, Black DM, Stamp GW, Solomon E, Trowsdale J. Very frequent loss of heterozygosity throughout chromosome 17 in sporadic ovarian carcinoma. *Int J Cancer* 1993; **54**: 220–225.

4 Pieretti M, Cavalieri C, Conway PS, Gallion HH, Powell DE, Turker MS. Genetic alterations distinguish different types of ovarian tumors. *Int J Cancer* 1995; **64**: 434–440.

5 Mitelman Database of Chromosome Aberrations in Cancer [database on the Internet]. 2007, Available from http://cgap.nci.nih.gov/Chromosomes/Mitelman.

6 Cao Q, Abeysinghe H, Chow O, Xu J, Kaung H, Fong C et al. Suppression of tumorigenicity in human ovarian carcinoma cell line SKOV-3 by microcell-mediated transfer of chromosome 11. *Cancer Genet Cytogenet* 2001; **129**: 131–137.

7 Salani R, Kurman RJ, Giuntoli 2nd R, Gardner G, Bristow R, Wang TL et al. Assessment of TP53 mutation using purified tissue samples of ovarian serous carcinomas reveals a higher mutation rate than previously reported and does not correlate with drug resistance. *Int J Gynecol Cancer* 2008; **18**: 487–491.

8 Ahmed AA, Etemadmoghadam D, Temple J, Lynch AG, Riad M, Sharma R et al. Driver mutations in TP53 are ubiquitous in high grade serous carcinoma of the ovary. *J Pathol* 2010; **221**: 49–56.

9 Miki Y, Swensen J, Shattuck-Eidens D, Futreal PA, Harshman K, Tavtigian S et al. A strong candidate for the breast and ovarian cancer susceptibility gene BRCA1. *Science* 1994; **266**: 66–71.

10 Easton DF, Ford D, Bishop DT. Breast and ovarian cancer incidence in BRCA1-mutation carriers. Breast Cancer Linkage Consortium. *Am J Hum Genet* 1995; **56**: 265–271.

11 Ford D, Easton DF, Bishop DT, Narod SA, Goldgar DE. Risks of cancer in BRCA1-mutation carriers. Breast Cancer Linkage Consortium. *Lancet* 1994; **343**: 692–695.

12 Wilcox CB, Baysal BE, Gallion HH, Strange MA, DeLoia JA. High-resolution methylation analysis of the BRCA1 promoter in ovarian tumors. *Cancer Genet Cytogenet* 2005; **159**: 114–122.

13 Baldwin RL, Nemeth E, Tran H, Shvartsman H, Cass I, Narod S et al. BRCA1 promoter region hypermethylation in ovarian carcinoma: a population-based study. *Cancer Res* 2000; **60**: 5329–5333.

14 Sangha N, Wu R, Kuick R, Powers S, Mu D, Fiander D et al. Neurofibromin 1 (NF1) defects are common in human ovarian serous carcinomas and co-occur with TP53 mutations. *Neoplasia* 2008; **10**: 1362–1372.

15 Feng Q, Deftereos G, Hawes SE, Stern JE, Willner JB, Swisher EM et al. DNA hypermethylation, Her-2/neu overexpression and p53 mutations in ovarian carcinoma. *Gynecol Oncol* 2008; **111**: 320–329.

16 Rathi A, Virmani AK, Schorge JO, Elias KJ, Maruyama R, Minna JD et al. Methylation profiles of sporadic ovarian tumors and nonmalignant ovaries from high-risk women. *Clin Cancer Res* 2002; **8**: 3324–3331.

17 Pergolizzi R, Appierto V, Crosti M, Cavadini E, Cleris L, Guffanti A et al. Role of retinoic acid receptor overexpression in sensitivity to fenretinide and tumorigenicity of human ovarian carcinoma cells. *Int J Cancer* 1999; **81**: 829–834.

18 Wojnarowicz PM, Provencher DM, Mes-Masson AM, Tonin PN. Chromosome 17q25 genes, RHBDF2 and CYGB, in ovarian cancer. *Int J Oncol* 2012; **40**: 1865–1880.

19 Wojnarowicz PM, Breznan A, Arcand SL, Filali-Mouhim A, Provencher DM, Mes-Masson AM et al. Construction of a chromosome 17 transcriptome in serous ovarian cancer identifies differentially expressed genes. *Int J Gynecol Cancer* 2008; **18**: 963–975.

20 Arnold JM, Huggard PR, Cummings M, Ramm GA, Chenevix-Trench G. Reduced expression of chemokine (C-C motif) ligand-2 (CCL2) in ovarian adenocarcinoma. *Br J Cancer* 2005; **92**: 2024–2031.

21 Negus RP, Stamp GW, Hadley J, Balkwill FR. Quantitative assessment of the leukocyte infiltrate in ovarian cancer and its relationship to the expression of C-C chemokines. *Am J Pathol* 1997; **150**: 1723–1734.

22 Negus RP, Stamp GW, Relf MG, Burke F, Malik ST, Bernasconi S et al. The detection and localization of monocyte chemoattractant protein-1 (MCP-1) in human ovarian cancer. *J Clin Invest* 1995; **95**: 2391–2396.

23 Goode EL, Maurer MJ, Sellers TA, Phelan CM, Kalli KR, Fridley BL et al. Inherited determinants of ovarian cancer survival. *Clin Cancer Res* 2010; **16**: 995–1007.

24 Fader AN, Rasool N, Vaziri SA, Kozuki T, Faber PW, Elson P et al. CCL2 expression in primary ovarian carcinoma is correlated with chemotherapy response and survival outcomes. *Anticancer Res* 2010; **30**: 4791–4798.

25 Rollins BJ. MCP-1, -2, -3, -4, -5. In: Oppenheim SF JJ, Durum S, Hirano T, Vilcek J, Nicola N (eds). *Cytokine Reference*. Academic Press: London, 2000, p 1145–1160.

26 Kuroda T, Kitadai Y, Tanaka S, Yang X, Mukaida N, Yoshihara M et al. Monocyte chemoattractant protein-1 transfection induces angiogenesis and tumorigenesis of gastric carcinoma in nude mice via macrophage recruitment. *Clin Cancer Res* 2005; **11**: 7629–7636.

27 Rollins BJ, Sunday ME. Suppression of tumor formation *in vivo* by expression of the JE gene in malignant cells. *Mol Cell Biol* 1991; **11**: 3125–3131.

28 Nesbit M, Schaider H, Miller TH, Herlyn M. Low-level monocyte chemoattractant protein-1 stimulation of monocytes leads to tumor formation in nontumorigenic melanoma cells. *J Immunol* 2001; **166**: 6483–6490.

29 Cody NA, Ouellet V, Manderson EN, Quinn MC, Filali-Mouhim A, Tellis P *et al.* Transfer of chromosome 3 fragments suppresses tumorigenicity of an ovarian cancer cell line monoallelic for chromosome 3. *Oncogene* 2007; **26**: 618–632.

30 Quinn MC, Filali-Mouhim A, Provencher DM, Mes-Masson AM, Tonin PN. Reprogramming of the transcriptome in a novel chromosome 3 transfer tumor suppressor ovarian cancer cell line model affected molecular networks that are characteristic of ovarian cancer. *Mol Carcinog* 2009; **48**: 648–661.

31 Provencher DM, Lounis H, Champoux L, Tetrault M, Manderson EN, Wang JC *et al.* Characterization of four novel epithelial ovarian cancer cell lines. *In Vitro Cell Dev Biol Anim* 2000; **36**: 357–361.

32 Zietarska M, Maugard CM, Filali-Mouhim A, Alam-Fahmy M, Tonin PN, Provencher DM *et al.* Molecular description of a 3D *in vitro* model for the study of epithelial ovarian cancer (EOC). *Mol Carcinog* 2007; **46**: 872–885.

33 Arcand SL, Provencher D, Mes-Masson AM, Tonin PN. OGG1 Cys326 variant, allelic imbalance of chromosome band 3p25.3 and TP53 mutations in ovarian cancer. *Int J Oncol* 2005; **27**: 1315–1320.

34 Quinn MC, Wilson DJ, Young F, Dempsey AA, Arcand SL, Birch AH *et al.* The chemiluminescence based Ziplex automated workstation focus array reproduces ovarian cancer Affymetrix GeneChip expression profiles. *J Transl Med* 2009; **7**: 55.

35 Zorn KK, Jazaeri AA, Awtrey CS, Gardner GJ, Mok SC, Boyd J *et al.* Choice of normal ovarian control influences determination of differentially expressed genes in ovarian cancer expression profiling studies. *Clin Cancer Res* 2003; **9**: 4811–4818.

36 Dubeau L. The cell of origin of ovarian epithelial tumors and the ovarian surface epithelium dogma: does the emperor have no clothes? *Gynecol Oncol* 1999; **72**: 437–442.

37 Auersperg N, Wong AS, Choi KC, Kang SK, Leung PC. Ovarian surface epithelium: biology, endocrinology, and pathology. *Endocr Rev* 2001; **22**: 255–288.

38 Salvador S, Gilks B, Kobel M. Huntsman D, Rosen B, Miller D. The fallopian tube: primary site of most pelvic high-grade serous carcinomas. *Int J Gynecol Cancer* 2009; **19**: 58–64.

39 Nokihara H, Yanagawa H, Nishioka Y, Yano S, Mukaida N, Matsushima K *et al.* Natural killer cell-dependent suppression of systemic spread of human lung adenocarcinoma cells by monocyte chemoattractant protein-1 gene transfection in severe combined immunodeficient mice. *Cancer Res* 2000; **60**: 7002–7007.

40 Sevko AL, Barysik N, Perez L, Shurin MR, Gerein V. Differences in dendritic cell activation and distribution after intravenous, intraperitoneal, and subcutaneous injection of lymphoma cells in mice. *Adv Exp Med Biol* 2007; **601**: 257–264.

41 Keyes KA, Mann L, Teicher B, Alvarez E. Site-dependent angiogenic cytokine production in human tumor xenografts. *Cytokine* 2003; **21**: 98–104.

42 Bodey B. Cancer-testis antigens: promising targets for antigen directed anti-neoplastic immunotherapy. *Expert Opin Biol Ther* 2002; **2**: 577–584.

43 Granot Z, Henke E, Comen EA, King TA, Norton L, Benezra R. Tumor entrained neutrophils inhibit seeding in the premetastatic lung. *Cancer Cell* 2011; **20**: 300–314.

44 Rollins BJ. Chemokines. *Blood* 1997; **90**: 909–928.

45 Chew V, Chen J, Lee D, Loh E, Lee J, Lim KH *et al.* Chemokine-driven lymphocyte infiltration: an early intratumoural event determining long-term survival in resectable hepatocellular carcinoma. *Gut* 2012; **61**: 427–438.

46 Dunn GP, Old LJ, Schreiber RD. The three Es of cancer immunoediting. *Annu Rev Immunol* 2004; **22**: 329–360.

47 Zitvogel L, Kroemer G. Introduction: the immune response against dying cells. *Curr Opin Immunol* 2008; **20**: 501–503.

48 Mok SC, Chan WY, Wong KK, Muto MG, Berkowitz RS. SPARC, an extracellular matrix protein with tumor-suppressing activity in human ovarian epithelial cells. *Oncogene* 1996; **12**: 1895–1901.

49 Charo IF, Myers SJ, Herman A, Franci C, Connolly AJ, Coughlin SR. Molecular cloning and functional expression of two monocyte chemoattractant protein 1 receptors reveals alternative splicing of the carboxyl-terminal tails. *Proc Natl Acad Sci USA* 1994; **91**: 2752–2756.

50 Neote K, DiGregorio D, Mak JY, Horuk R, Schall TJ. Molecular cloning, functional expression, and signaling characteristics of a C-C chemokine receptor. *Cell* 1993; **72**: 415–425.

51 Schecter AD, Berman AB, Yi L, Ma H, Daly CM, Soejima K *et al.* MCP-1-dependent signaling in CCR2(-/-) aortic smooth muscle cells. *J Leukoc Biol* 2004; **75**: 1079–1085.

52 Heesen M, Tanabe S, Berman MA, Yoshizawa I, Luo Y, Kim RJ *et al.* Mouse astrocytes respond to the chemokines MCP-1 and KC, but reverse transcriptase-polymerase chain reaction does not detect mRNA for the KC or new MCP-1 receptor. *J Neurosci Res* 1996; **45**: 382–391.

53 Fahey JV, Schaefer TM, Channon JY, Wira CR. Secretion of cytokines and chemokines by polarized human epithelial cells from the female reproductive tract. *Hum Reprod* 2005; **20**: 1439–1446.

54 TCGA. Integrated genomic analyses of ovarian carcinoma. *Nature* 2011; **474**: 609–615.

55 Lounis H, Provencher D, Godbout C, Fink D, Milot MJ, Mes-Masson AM. Primary cultures of normal and tumoral human ovarian epithelium: a powerful tool for basic molecular studies. *Exp Cell Res* 1994; **215**: 303–309.

56 Therasse P, Arbuck SG, Eisenhauer EA, Wanders J, Kaplan RS, Rubinstein L *et al.* New guidelines to evaluate the response to treatment in solid tumors. European Organization for Research and Treatment of Cancer, National Cancer Institute of the United States, National Cancer Institute of Canada. *J Natl Cancer Inst* 2000; **92**: 205–216.

57 Ouellet V, Zietarska M, Portelance L, Lafontaine J, Madore J, Puiffe ML *et al.* Characterization of three new serous epithelial ovarian cancer cell lines. *BMC Cancer* 2008; **8**: 152.

58 Kruk PA, Maines-Bandiera SL, Auersperg N. A simplified method to culture human ovarian surface epithelium. *Lab Invest* 1990; **63**: 132–136.

59 Presneau N, Mes-Masson AM, Ge B, Provencher D, Hudson TJ, Tonin PN. Patterns of expression of chromosome 17 genes in primary cultures of normal ovarian surface epithelia and epithelial ovarian cancer cell lines. *Oncogene* 2003; **22**: 1568–1579.

60 Presneau N, Dewar K, Forgetta V, Provencher D, Mes-Masson AM, Tonin PN. Loss of heterozygosity and transcriptome analyses of a 1.2 Mb candidate ovarian cancer tumor suppressor locus region at 17q25.1-q25.2. *Mol Carcinog* 2005; **43**: 141–154.

61 Rozen S, Skaletsky H. Primer3 on the WWW for general users and for biologist programmers. *Methods Mol Biol* 2000; **132**: 365–386.

62 Karolchik D, Baertsch R, Diekhans M, Furey TS, Hinrichs A, Lu YT *et al.* The UCSC Genome Browser Database. *Nucleic Acids Res* 2003; **31**: 51–54.

63 Arcand SL, Maugard CM, Ghadirian P, Robidoux A, Perret C, Zhang P *et al.* Germline TP53 mutations in BRCA1 and BRCA2 mutation-negative French Canadian breast cancer families. *Breast Cancer Res Treat* 2008; **108**: 399–408.

64 Kelm JM, Timmins NE, Brown CJ, Fussenegger M, Nielsen LK. Method for generation of homogeneous multicellular tumor spheroids applicable to a wide variety of cell types. *Biotechnol Bioeng* 2003; **83**: 173–180.

65 Arcand SL, Mes-Masson AM, Provencher D, Hudson TJ, Tonin PN. Gene expression microarray analysis and genome databases facilitate the characterization of a chromosome 22 derived homogeneously staining region. *Mol Carcinog* 2004; **41**: 17–38.

66 Novak JP, Sladek R, Hudson TJ. Characterization of variability in large-scale gene expression data: implications for study design. *Genomics* 2002; **79**: 104–113.

67 Dennis Jr G, Sherman BT, Hosack DA, Yang J, Gao W, Lane HC *et al.* DAVID: database for annotation, visualization, and integrated discovery. *Genome Biol* 2003; **4**: P3.

Supplementary Information accompanies the paper on the Oncogenesis website (http://www.nature.com/oncsis).